

# PIN FORMED 2 Modulates the Transport of Arsenite in *Arabidopsis thaliana*

Mohammad Arif Ashraf<sup>1,11</sup>, Kana Umetsu<sup>2,11</sup>, Olena Ponomarenko<sup>3,11</sup>, Michiko Saito<sup>2</sup>, Mohammad Aslam<sup>2</sup>, Olga Antipova<sup>4</sup>, Natalia Dolgova<sup>3</sup>, Cheyenne D. Kiani<sup>3,12,13</sup>, Susan Nezhati<sup>3</sup>, Keitaro Tanoi<sup>5</sup>, Katsuyuki Minegishi<sup>6</sup>, Kotaro Nagatsu<sup>6</sup>, Takehiro Kamiya<sup>7</sup>, Toru Fujiwara<sup>7</sup>, Christian Luschnig<sup>8</sup>, Karen Tanino<sup>9</sup>, Ingrid Pickering<sup>3</sup>, Graham N. George<sup>3</sup> and Abidur Rahman<sup>1,2,10,\*</sup>

<sup>1</sup>United Graduate School of Agricultural Sciences, Iwate University, Morioka, Iwate, Japan

<sup>2</sup>Department of Plant Bio Sciences, Faculty of Agriculture, Iwate University, Morioka, Iwate, Japan

<sup>3</sup>Molecular and Environmental Science Research Group, Department of Geological Sciences, University of Saskatchewan, Saskatoon, SK, Canada

<sup>4</sup>Argonne National Lab, Advanced Photon Source, XSD-MIC, Lemont, IL, USA

<sup>5</sup>Isotope Facility for Agricultural Education and Research, Graduate School of Agricultural and Life Sciences, The University of Tokyo, Bunkyo-ku, Tokyo, Japan

<sup>6</sup>Department of Radiopharmaceuticals Development, National Institute of Radiological Sciences, National Institutes for Quantum and Radiological Science and Technology, Inage, Chiba, Japan

<sup>7</sup>Department of Applied Biological Chemistry, Graduate School of Agricultural and Life Sciences, The University of Tokyo, Bunkyo-ku, Tokyo, Japan

<sup>8</sup>Department of Applied Genetics and Cell Biology, University of Natural Resources and Life Sciences, Vienna (BOKU), Muthgasse 18, 1180 Wien, Austria

<sup>9</sup>Department of Plant Sciences, College of Agriculture and Bioresources, University of Saskatchewan, Saskatoon, SK, Canada

<sup>10</sup>Agri-Innovation Center, Iwate University, Morioka, Iwate, Japan

<sup>11</sup>These authors contributed equally to this article.

<sup>12</sup>Present address: Biological Sciences, 507 Campus Drive NW, Calgary, AB, Canada

<sup>13</sup>Present address: University of Calgary, 2500 University Drive NW, Calgary, AB T2N 1N4, Canada

\*Correspondence: Abidur Rahman ([abidur@iwate-u.ac.jp](mailto:abidur@iwate-u.ac.jp))

<https://doi.org/10.1016/j.xplc.2019.100009>

## ABSTRACT

**Arsenic contamination is a major environmental issue, as it may lead to serious health hazard. The reduced trivalent form of inorganic arsenic, arsenite, is in general more toxic to plants compared with the fully oxidized pentavalent arsenate. The uptake of arsenite in plants has been shown to be mediated through a large subfamily of plant aquaglyceroporins, nodulin 26-like intrinsic proteins (NIPs). However, the efflux mechanisms, as well as the mechanism of arsenite-induced root growth inhibition, remain poorly understood. Using molecular physiology, synchrotron imaging, and root transport assay approaches, we show that the cellular transport of trivalent arsenicals in *Arabidopsis thaliana* is strongly modulated by PIN FORMED 2 (PIN2) auxin efflux transporter. Root transport assay using radioactive arsenite, X-ray fluorescence imaging (XFI) coupled with X-ray absorption spectroscopy (XAS), and inductively coupled plasma mass spectrometry analysis revealed that *pin2* plants accumulate higher concentrations of arsenite in roots compared with the wild-type. At the cellular level, arsenite specifically targets intracellular sorting of PIN2 and thereby alters the cellular auxin homeostasis. Consistently, loss of PIN2 function results in arsenite hypersensitivity in roots. XFI coupled with XAS further revealed that loss of PIN2 function results in specific accumulation of arsenical species, but not the other metals such as iron, zinc, or calcium in the root tip. Collectively, these results suggest that PIN2 likely functions as an arsenite efflux transporter for the distribution of arsenical species *in planta*.**

**Key words:** auxin, arsenite, PIN2, trafficking, transport

Ashraf M.A., Umetsu K., Ponomarenko O., Saito M., Aslam M., Antipova O., Dolgova N., Kiani C.D., Nezhati S., Tanoi K., Minegishi K., Nagatsu K., Kamiya T., Fujiwara T., Luschnig C., Tanino K., Pickering I., George G.N., and Rahman A. (2019). PIN FORMED 2 Modulates the Transport of Arsenite in *Arabidopsis thaliana*. Plant Comm. ■ ■, 100009.

Published by the Plant Communications Shanghai Editorial Office in association with Cell Press, an imprint of Elsevier Inc., on behalf of CSPB and IPPE, SIBS, CAS.

## INTRODUCTION

It is estimated that more than 140 million people worldwide are affected by the elevated levels of arsenic (As) in drinking water (WHO, 2018, <https://www.who.int/news-room/fact-sheets/detail/arsenic>). Plants readily accumulate arsenic from contaminated soils and irrigation water, resulting in arsenic exposure to population, especially in arsenicosis-affected areas where irrigated crops are the main staple of the diet (Meharg and Zhao, 2012). Breeding of resistant crop varieties with low accumulation of arsenic requires understanding of complex molecular interactions involved in arsenic uptake, biotransformation, compartmentalization, and extrusion mechanisms in plants.

Arsenic has a range of oxidation states from  $-3$  to  $+5$  and forms a large variety of organic and inorganic compounds. In natural aquifers the arsenic oxyanions, pentavalent arsenates (iAs(V)) and reduced trivalent arsenites (iAs(III)), are predominant inorganic species in aerobic and anaerobic environments, respectively. Trivalent arsenicals are regarded to be more toxic compared to their pentavalent analogs. The toxicity of trivalent arsenicals is connected to their propensity of binding to sulfhydryl groups of proteins, resulting in disruption of redox processes and the metabolism of a cell as a whole (Shen et al., 2013). Over a broad range of pH values ( $pK_a = 9.2$ ), solvated iAs(III) species is present as an uncharged non-dissociated  $As(OH)_3$  polyol molecule, which structurally and chemically resembles glycerol (Ravenscroft et al., 2009; Yang et al., 2012). Like microorganisms and mammalian cells, higher plants also use aquaglyceroporin proteins to facilitate arsenite entry into plant root cells. It was shown that three of the five plant aquaporin subfamilies, namely NIPs (nodulin 26-like intrinsic proteins), PIPs (plasma membrane intrinsic proteins), and TIPs (tonoplast intrinsic proteins), are involved in the uptake and translocation of iAs(III) species and methylated organic arsenic metabolites in plant cells and tonoplasts, respectively. Many aquaporins demonstrate bidirectional transport properties for arsenic species, so their action can result in cellular efflux of the arsenic into the apoplast (Maciaszczyk-Dziubinska et al., 2012; Xu et al., 2015).

In aerobic conditions, the plant phosphate transporters are the main channel of inorganic As(V) species' uptake into the cell, where they interfere with processes of oxidative phosphorylation (Shen et al., 2013; Latowski et al., 2018). Inside the plant cell, As(V) is readily reduced to As(III) species with the help of arsenate reductases, of ACR2 and HAC1 (Ellis et al., 2006; Salt, 2017). As-hyperaccumulating ferns from the *Pteris* genus make use of ACR3-like transporters, absent in angiosperms, to accumulate inorganic arsenite in vacuoles of shoot tissues and gametophytes, possibly as a defense against herbivores (Indriolo et al., 2010). In angiosperms, however, one of the main detoxification mechanisms is formation of As(III) complexes with sulfhydryl (-SH) groups in glutathione and cysteine-rich polypeptides, plant phytochelatin (PCs), and metallothioneins, which are sequestered in the vacuoles with the help of ABCC transporters (Pickering et al., 2000; Shen et al., 2013; Song et al., 2014). Reduction of As(V) to As(III) was also shown to facilitate excretion of arsenicals back to the external medium (Chen et al., 2013). Furthermore, it has been found that non-hyperaccumulating species store a major-

ity of As(III)-thiolated species in root vacuoles (Latowski et al., 2018).

Arsenite loading and transport into the root vascular system are found to be modulated by several transporters. In *Arabidopsis*, AtNIP1;1 and AtNIP3;1, and in rice, OsNIP2;1 (Lsi1) have been characterized as major arsenite uptake carriers (Ma et al., 2008; Kamiya et al., 2009; Xu et al., 2015). The efflux of arsenite from exodermis and endodermis cells to the xylem in rice roots is suggested to be largely regulated by a silicon efflux carrier, Lsi2 (Ma et al., 2008). Recently, involvement of the auxin transporter, AUX1, in arsenite response has been shown. The plant tolerance to arsenite is linked to AUX1-mediated auxin transport and reactive oxygen species (ROS)-mediated signaling (Krishnamurthy and Rathinasabapathi, 2013). However, a potential role of auxin transporters in arsenite transport was not investigated.

The family of PIN FORMED (PINs) are transporters that facilitate cellular auxin redistribution and homeostasis that directly affects plant growth and development under both optimal and stressed conditions (Okada et al., 1991; Luschnig et al., 1998; Shibasaki et al., 2009; Hanzawa et al., 2013; Wu et al., 2015; Ashraf and Rahman, 2019). Sequence alignments and phylogenetic comparisons position PIN proteins as a part of the bile/arsenite/riboflavin transporter (BART) superfamily of secondary transporters and signaling proteins (Mansour et al., 2007). Notably, members of BART include the Arc3 family of arsenical resistance bacterial proteins transporting As(III) and Sb(III) (Maciaszczyk-Dziubinska et al., 2012).

In several instances, protein activities are not confined to only one function. For example, LSi2, a plasma membrane silicic acid efflux pump, is also a member of the Arsenite-Antimonite (ArsB) efflux family, and serves as an arsenite efflux transporter in plants (Ma et al., 2008). In this respect, LSi2 shows 18% identity with the *Escherichia coli* efflux transporter ArsB (Ma et al., 2008). Although these two transporters from two different species show very low sequence identity, they execute a similar function at the cellular level, raising the possibility that other plant transporters homologous to ArsB may show related functionality. In fact, it was previously reported that hydrophobic domains of the auxin efflux facilitator EIR1/PIN FORMED 2 (PIN2) show up to 35%–40% similarity to *E. coli* efflux carrier ArsB, and to SbmA, an *E. coli* integral membrane protein, which is required for the uptake of the antibiotic Microcin 25 (Luschnig et al., 1998).

Although PIN2 shows a higher homology to ArsB compared with Lsi2, no effort has been made to characterize whether PIN2 plays any functional role in arsenite transport. Using physiology, molecular and cell biology, high-resolution synchrotron imaging, and root transport assay approaches, we tried to decipher the role of PINs in regulating arsenic response. Our results demonstrate that: (1) the arsenite, but not the arsenate, response in *Arabidopsis* root depends on PIN2; (2) arsenite alters intracellular auxin homeostasis through selective modulation of PIN2 trafficking; (3) loss of PIN2 specifically affects the accumulation of arsenical species, but not of the other metals such as zinc, iron, or calcium in the *Arabidopsis* root tip; and (4) PIN2 facilitates the transport of trivalent arsenical species and potentially participates in the efflux of arsenite metabolites *in planta*.

	SsAcr3	PvAcr3	arsB	OsLsi2	AtPIN2	AtPIN1	AtPIN3
SsAcr3	100.00	40.16	8.22	6.44	16.67	18.01	17.28
PvAcr3	40.16	100.00	13.99	6.86	17.65	18.45	18.13
arsB	8.22	13.99	100.00	12.15	24.51	24.44	24.86
OsLsi2	6.44	6.86	12.15	100	10.26	9.63	8.83
AtPIN2	16.67	17.65	24.51	10.26	100.00	62.88	60.88
AtPIN1	18.01	18.45	24.44	9.63	62.88	100.00	65.49
AtPIN3	17.28	18.13	24.86	8.83	60.88	65.49	100.00

**Table 1. Homology of Plant Auxin Efflux Carrier (PINs) and Arsenite Transporters.**

Identity matrix of *Saccharomyces cerevisiae* Acr3 (SsAcr3), *Pteris vittata* Acr3 (PvAcr3) and *Escherichia coli* arsenite transporter (arsB), *Oryza sativa* silicon transporter (OsLsi2), and *Arabidopsis thaliana* PINs (AtPIN1, AtPIN2, AtPIN3).

## RESULTS

### Homology of Plant Auxin Efflux Carriers and Selected Arsenite Transporters

Previously it was reported that portions of PIN2 show 35%–40% identity to the bacterial transporter ArsB (Luschnig et al., 1998). We reassessed the homology of PIN proteins with different arsenite transporters using a bioinformatics approach. Plasma membrane-localized PIN proteins, which function as intracellular auxin efflux carriers, all have a similar structure, with two hydrophobic domains, consisting of about five transmembrane helices each, separated by a central intracellular hydrophilic domain. Among the eight annotated PIN proteins in *Arabidopsis*, PIN1, PIN2, PIN3, PIN4, and PIN7 reside in the plasma membrane, while PIN5 and PIN8 are localized in the endoplasmic reticulum (ER). Recent research showed a complex behavior and localization of PIN6 both in ER and plasma membrane (Simon et al., 2016).

The cladogram of the plasma membrane-localized PIN proteins places PIN1 and PIN2 in one clade, and PIN3, PIN4, and PIN7 in another clade, where PIN3 and PIN7 are closely associated because of their high homology (Supplemental Figure 1). In general, the homology among plasma membrane-residing PIN proteins ranges from 60% to 90% (Supplemental Figure 2 and Supplemental Table 1). Multiple sequence alignments of PIN1, PIN2, and PIN3 proteins against various arsenite transporters revealed that they show approximately 25% homology with bacterial transporter ArsB, but lower homology with Lsi2 (Table 1, Supplemental Figure 3, and Supplemental Table 2). AtPINs also showed 18% homology to arsenite transporters Acr3 from yeast *Saccharomyces cerevisiae* (Ghosh et al., 2002) and arsenic hyperaccumulator fern *Pteris vittata* (Indriolo et al., 2010). Compared with Lsi2, AtPINs show higher homology to all the known arsenite transporters (Table 1 and Supplemental Table 3).

### Loss of PIN2 Function Results in Altered Response to Arsenite

To understand the functional significance of AtPINs homology to bacterial arsenite transporter ArsB, we next investigated the response of selected *pin1*, *pin2*, *pin3*, and *pin4* mutants to both arsenite and arsenate. Root elongation in *Arabidopsis thaliana* shows a strong response to exogenous arsenite and arsenate, albeit at different concentrations. Time-course and dose-

response assays of root growth in wild-type revealed that approximately 50% inhibition of root elongation can be achieved with 10  $\mu$ M arsenite over 3 days of incubation (Figure 1A and 1B). Consistent with previous results (Lee et al., 2003), a much higher concentration of arsenate (1.5 mM) was required to achieve a similar degree of root elongation inhibition (Supplemental Figure 5).

Among the membrane-residing PIN mutants that were tested for root growth assay, the response of *pin2* to arsenite exposure was the most striking. At all tested concentrations of arsenite, two independent alleles of *pin2*, *eir1-4*, and *eir1-1* roots showed a hypersensitive response to arsenite-induced inhibition of root elongation. Additionally, roots of both alleles exhibited hook-like curling in the presence of arsenite (Figure 1C and 1D; Supplemental Figure 4). Since both alleles show essentially the same response, we focused on the more widely used allele *eri1-1* for subsequent experiments. Complementation of *pin2* mutation with genomic PIN2 reverted both the curling root phenotype and hypersensitive root growth response, confirming that the observed altered response of the *pin2* mutant toward arsenite is linked to PIN2 (Figure 1C and 1D). This is supported further by the finding that overexpression of PIN2 results in improved arsenite tolerance at all arsenite concentrations tested (Supplemental Figure 4). In contrast, all these mutants showed wild-type-like response to arsenate-induced root growth inhibition (Supplemental Figure 5). In a previous report, it was claimed that both *pin2* and *pin1* mutants were hypersensitive to arsenite-induced root growth inhibition (Krishnamurthy and Rathinasabapathi, 2013). However, in our screening, *pin1*, *pin3*, and *pin4* mutants showed a wild-type response to arsenite exposure (Figure 1C and 1D). Collectively, these results suggest that PIN2 functions as a potential regulator of arsenite response in roots.

### Arsenite Alters Auxin Response in *Arabidopsis* Roots through Modulating Auxin Transport

PIN2 functions in auxin efflux in the lateral root cap (LRC), epidermal, and cortex cells, and through its intracellular polarity it maintains a maximal auxin gradient at the root tip, which is an absolute requirement for the root gravity response (Rahman et al., 2010). Consistently, loss of PIN2 results in an agravitropic root growth phenotype (Luschnig et al., 1998). Since *pin2/eir1-1* showed altered response to arsenite, we hypothesized that arsenite may affect the root auxin response. To clarify this

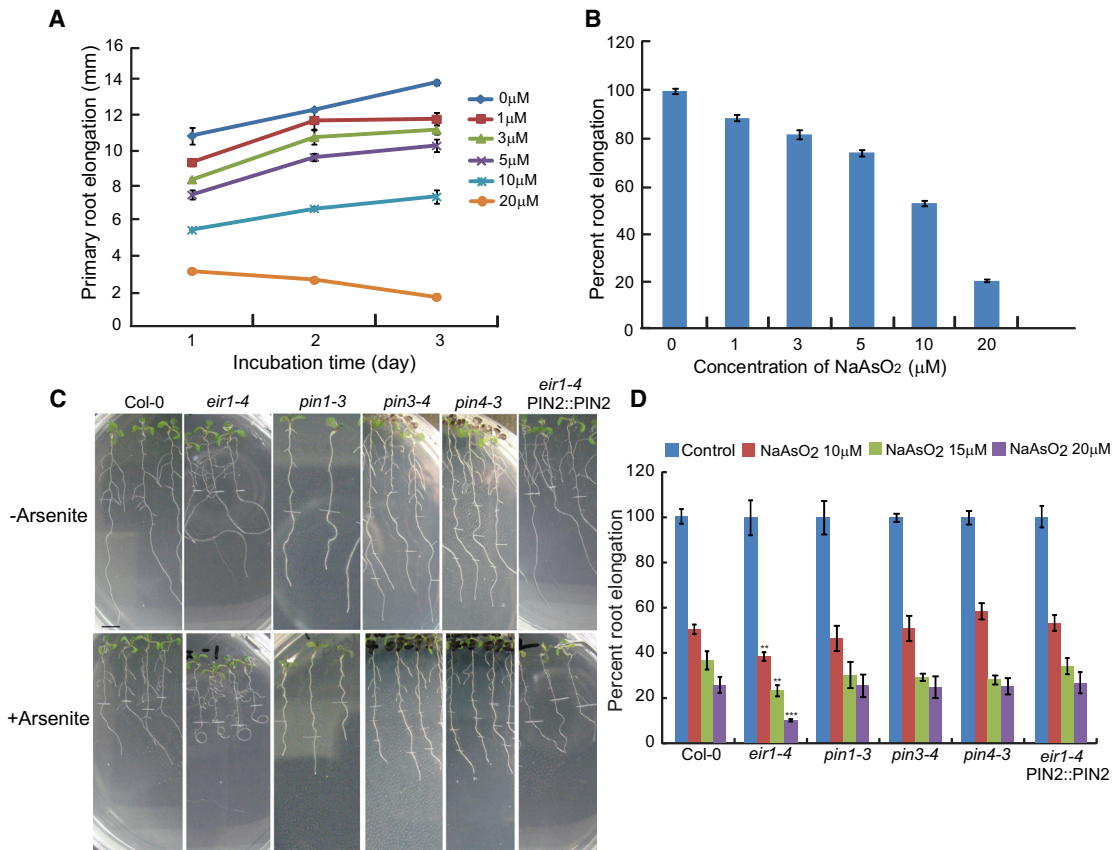


**Figure 1. Effect of Arsenite on Root Elongation Response.**

Five-day-old light-grown wild-type or mutant seedlings were transferred to new agar plates supplemented with or without arsenite and incubated for various lengths of time under continuous light.

(A) Time course of arsenite-induced inhibition of root elongation in wild type.

(B) Dose response of arsenite for root elongation in wild-type after 3-day incubation. Approximately 50% inhibition of root growth was observed at 10 μM arsenite.

(C) Representative images of root phenotype of wild-type, *pin* mutants, and *pin2* complemented line after 10 μM arsenite treatment for 3 days. Scale Bar represents 0.5 cm.

(D) *pin2/eir1-4* mutant shows hypersensitive response to arsenite-induced root growth inhibition. Five-day-old *Arabidopsis* seedlings were subjected to arsenite treatment for 3 days. Compared with wild-type, *eir1-4* showed hypersensitive response to arsenite-induced inhibition of root elongation at all concentrations we tested as judged by Student's *t*-test ( $P < 0.0001$ ), while complemented line of *pin2*, *eir1-4*-PIN2::PIN2 show wild-type-like response to arsenite-induced root growth inhibition.

For data shown in (A), (B), and (D), vertical bars represent mean ± SE of the experimental means from at least five independent experiments ( $n = 5$  or more), where experimental means were obtained from 8–10 seedlings per experiment.

possibility, we investigated the effect of arsenite on the root gravity response in wild-type roots. Arsenite considerably slows down the gravity response of the wildtype roots. Importantly, we observed such altered gravity responses during early stages of root bending, conditions under which arsenite exhibited no obvious effects on root elongation (Figure 2A and 2B), thus confirming that arsenite effects on the gravity response are not immediate consequences of compromised root elongation.

The root gravity response is regulated by the asymmetric distribution of auxin, which is largely dependent on the auxin efflux by PIN2 (Luschnig et al., 1998; Rahman et al., 2010). To understand whether the cellular auxin homeostasis in the root meristem is altered by arsenite, we monitored the intracellular auxin response using two auxin-responsive markers, *IAA2-GUS* and *DII-VENUS*, both of which are capable of detecting intracel-

lular auxin distribution/signaling at high spatiotemporal resolution (Luschnig et al., 1998; Shibasaki et al., 2009; Band et al., 2012; Brunoud et al., 2012; Hanzawa et al., 2013). Only a brief incubation in arsenite altered the auxin response pattern in root meristem. Specifically, a more intense β-glucuronidase (GUS) staining was observed in arsenite-treated roots compared with wild-type, and the response was proportional to the incubation time (Figure 2C and 2D). Similar results were observed with the *DII-VENUS* marker line in response to long-term arsenite treatment (Supplemental Figure 6). Interestingly, after 2 h of incubation in arsenite, GUS signal started to accumulate in the peripheral cell files, namely epidermis and cortex in root meristem (Figure 2C). Such GUS staining has previously been linked to inhibition of auxin transport (Shibasaki et al., 2009), indicating that arsenite may affect auxin transport. Consistently, assessment of shootward auxin transport (which is largely

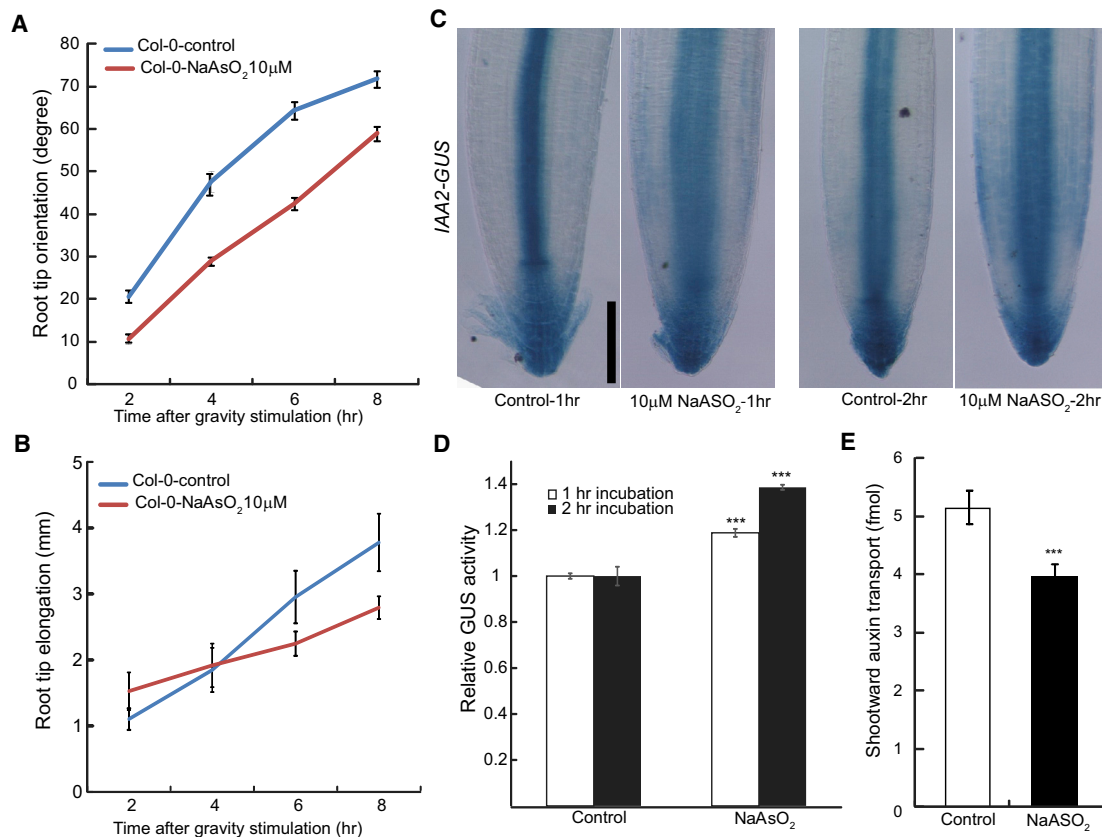


**Figure 2. Arsenite Inhibits Root Gravity, Alters Intracellular Auxin Response, and Inhibits Auxin Transport.**

**(A)** Effect of Arsenite on root gravity response. For assaying gravitropism, 5-day-old light-grown seedlings were transferred to arsenite and gravistimulated. Data for root tip orientation were collected for 2, 4, 6, and 8 h. Vertical bars represent mean  $\pm$  SE of the experimental means from at least five independent experiments ( $n = 5$  or more), where experimental means were obtained from 8–10 seedlings per experiment. Arsenite-induced inhibition of root gravity response was significant at all time points as judged by Student's  $t$ -test ( $P < 0.0001$ ).

**(B)** Effect of arsenite on root elongation during the gravity assay. Arsenite-induced root growth inhibition was insignificant at all time points as judged by Student's  $t$ -test.

**(C)** Arsenite alters the intracellular auxin response. Five-day-old light-grown *IAA2-GUS* seedlings were treated with 10  $\mu$ M arsenite for 1 h and 2 h. After the arsenite treatment, GUS staining was performed by incubating the seedlings in GUS staining buffer for 1 h at 37°C. Images are representative of 15–20 roots obtained from at least three independent experiments. Scale bar represents 100  $\mu$ m.

**(D)** Quantification of GUS activity obtained from experiment in **(C)**. Vertical bars represent mean  $\pm$  SE. Compared with the control treatment, arsenite-induced increase in GUS activity was highly significant as judged by Student's  $t$ -test ( $P < 0.0001$ ) at both time points as judged by Student's  $t$ -test.

**(E)** Effect of arsenite on shootward auxin transport. Five-day-old light-grown seedlings were transferred to new agar plates and subjected to arsenite treatment before transport of [<sup>3</sup>H]IAA over 2 h was measured as described in [Methods](#). The experiments were conducted using at least three biological replicates. For each biological replicate, three technical replicates were assayed. (Col-control,  $n = 57$ ; Col-arsenite,  $n = 52$ ). Asterisks represent the statistical significance between treatment as judged by Student's  $t$ -test ( $***P < 0.0001$ ). Vertical bars represent mean  $\pm$  SE of the experimental means.

regulated by PIN2) with <sup>3</sup>H-labeled indole-3-acetic acid (IAA) revealed that arsenite indeed inhibits the shootward auxin transport (Figure 2E).

These results suggest that in addition to other systemic effects likely caused by trivalent arsenicals in living cells (Shen et al., 2013), arsenite-modulated PIN2 activity resulted in altered cellular auxin response and reduced auxin transport.

### Arsenite Alters Intracellular Trafficking of PIN2

To provide a mechanistic explanation for arsenite effects on *pin2* mutant, we next investigated expression of PIN2 both at transcriptional and translational levels. The transcript analyses of PIN2 by quantitative real-time PCR revealed no significant differ-

ence in transcript levels upon arsenite treatment, suggesting that PIN2 is not under direct transcriptional regulation of arsenite (Supplemental Figure 7). Earlier it was demonstrated that for proper functioning of PIN2 as an IAA efflux protein, both the polar deployment and intracellular trafficking of PIN2 are required (Luschnig et al., 1998; Laxmi et al., 2008; Shibasaki et al., 2009; Wan et al., 2012; Hanzawa et al., 2013). Moreover, this trafficking process has also been shown to be sensitive to various kinds of stresses (Luschnig et al., 1998; Laxmi et al., 2008; Shibasaki et al., 2009; Wan et al., 2012; Hanzawa et al., 2013). Cellular localization of PIN2, using PIN2-green fluorescent protein (GFP) transgenic seedlings (Xu and Scheres, 2005) revealed that arsenite did not alter the asymmetric localization of PIN2 (Figure 3A, upper panel) but did interfere with protein trafficking (Figure 3B). In control wild-type plants, treatment

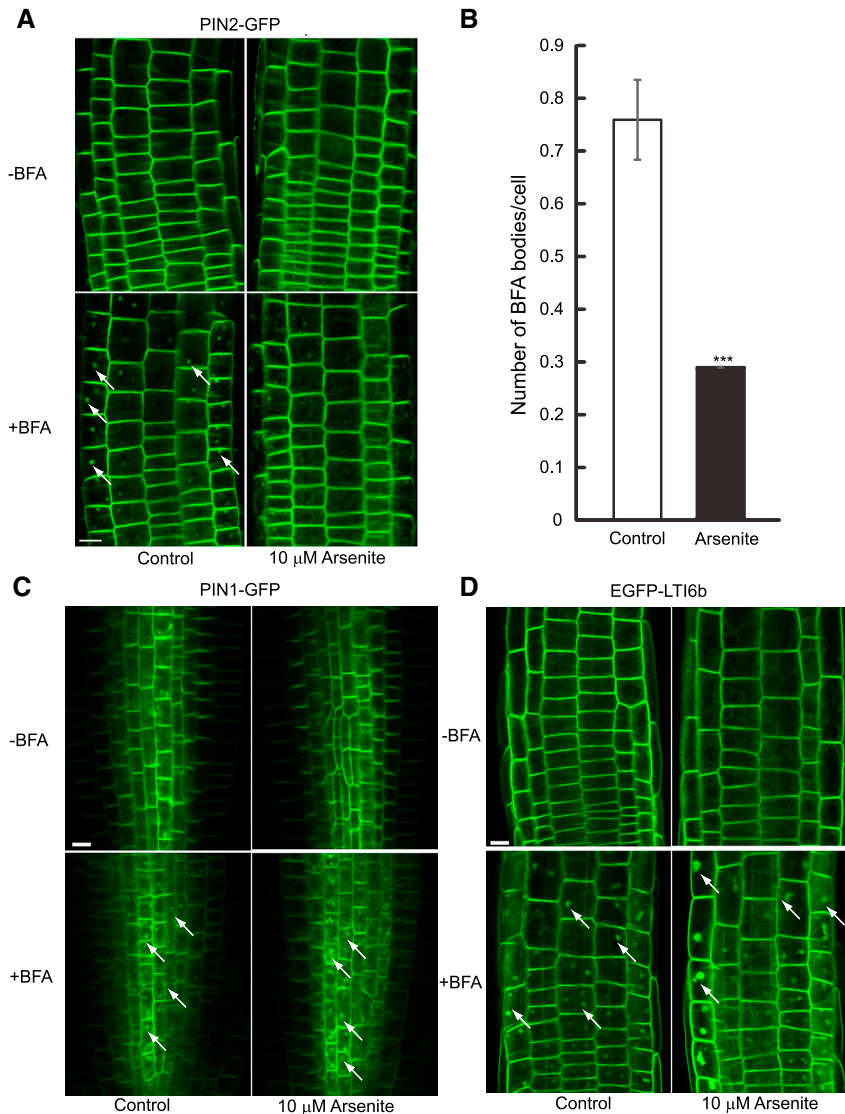


**Figure 3. Arsenite Specifically Affects the Intracellular Dynamic Cycling of PIN2.**

Five-day-old PIN2::PIN2-GFP, PIN1::PIN1-GFP, and EGFP-LTI6b transgenic seedlings were treated with arsenite for 2 h. After the incubation, seedlings were treated with 20 μM BFA for 40 min. The images were captured using same confocal setting and are representative of 15–20 roots obtained from at least four independent experiments. **(A)** Effect of arsenite on PIN2 trafficking. Scale bar represents 10 μm.

**(B)** Quantitative analysis of formation of PIN2-BFA body in the transition zone of PIN2::PIN2-GFP transgenic plants in presence or absence of arsenite. Total number of BFA bodies and number of cells were counted in the imaged area. Bar graph represents the average number of BFA bodies formed per cell. Vertical bars represent mean ± SE of the experimental means ( $n = 4$  or more). Asterisks represent the statistical significance between treatments as judged by Student's  $t$ -test ( $***P < 0.0001$ ).

**(C and D)** Effect of arsenite on PIN1 **(C)** and LTI6b **(D)** trafficking. Note that BFA bodies are formed in the presence of arsenite. Arrowheads indicate BFA bodies. Scale bar represents 10 μm.

### Arsenite Distribution Is Altered in *pin2* Roots

In bacteria and yeast, arsenite transport has been extensively studied. In yeast, arsenite is removed from the cells by Acr3, a plasma membrane-localized efflux carrier and some aquaglyceroporins, functioning as bidirectional arsenite transporters (Maciaszczyk-Dziubinska et al., 2012; Yang et al., 2012). In bacteria, arsenite uptake and efflux is passively regulated by the bidirectional aquaglyceroprotein channels and also pumped outside of the cells by ArsB or ArsAB functioning as  $\text{As}(\text{OH})_3\text{-H}^+$  antiporter or ATP-driven extrusion pump, respectively. Some bacteria possess both ArsAB and Acr3 efflux systems (Meharg and Zhao, 2012; Yang et al., 2012).

In plants, several aquaglyceroprotein NIPs have been shown to regulate passive, gradient-driven arsenite uptake, while only a single protein, rice Lsi2, has been implicated in active regulation of arsenite efflux. Rice Lsi2 is a silicon transporter and shows 18% homology to the bacterial arsenite transporter, ArsB (Ma et al., 2008; Meharg and Zhao, 2012). PIN2 shows a higher homology to ArsB, which together with arsenite effects on *pin2/eir1-1* roots and on PIN2 trafficking led us to hypothesize that PIN2 may mediate arsenite transport in roots as well. To test this possibility, we combined  $^{74,73}\text{As}(\text{III})$  root transport assay, inductively coupled plasma mass spectrometry (ICP-MS) analysis of arsenic accumulation, and speciation and localization of arsenic in roots using high-resolution synchrotron X-ray fluorescence imaging (XFI) analysis coupled with X-ray absorption spectroscopy (XAS).

with Brefeldin A (BFA), an inhibitor of anterograde PIN trafficking (Geldner et al., 2001), resulted in formation of large number of PIN2-positive small bodies in the cytosol, indicative of disturbed (re)cycling of PIN2 between the plasma membrane and endosomal compartments (Figure 3A and Supplemental Figure 8). In contrast, formation of these small PIN2-positive bodies was drastically reduced, in response to both short (2 h) and long-term (3 days) arsenite treatments (Figure 3A and 3B; Supplemental Figure 8A and 8B), suggesting that elevated arsenite levels impact on the intracellular sorting of PIN2.

To elucidate the specificity of arsenite-induced inhibition of PIN2 trafficking, we investigated its effect on the trafficking of PIN1, a close homolog of PIN2 and LTI6b, a cold-inducible membrane protein, which is trafficked from the plasma membrane to endosomes through a BFA-regulated pathway (Kurup et al., 2005; Shibasaki et al., 2009). Both short- and long-term arsenite treatments resulted in formation of BFA-induced PIN1 and LTI6b bodies (Figure 3C and 3D; Supplemental Figure 8C and 8D), suggesting that arsenite specifically targets PIN2 trafficking.

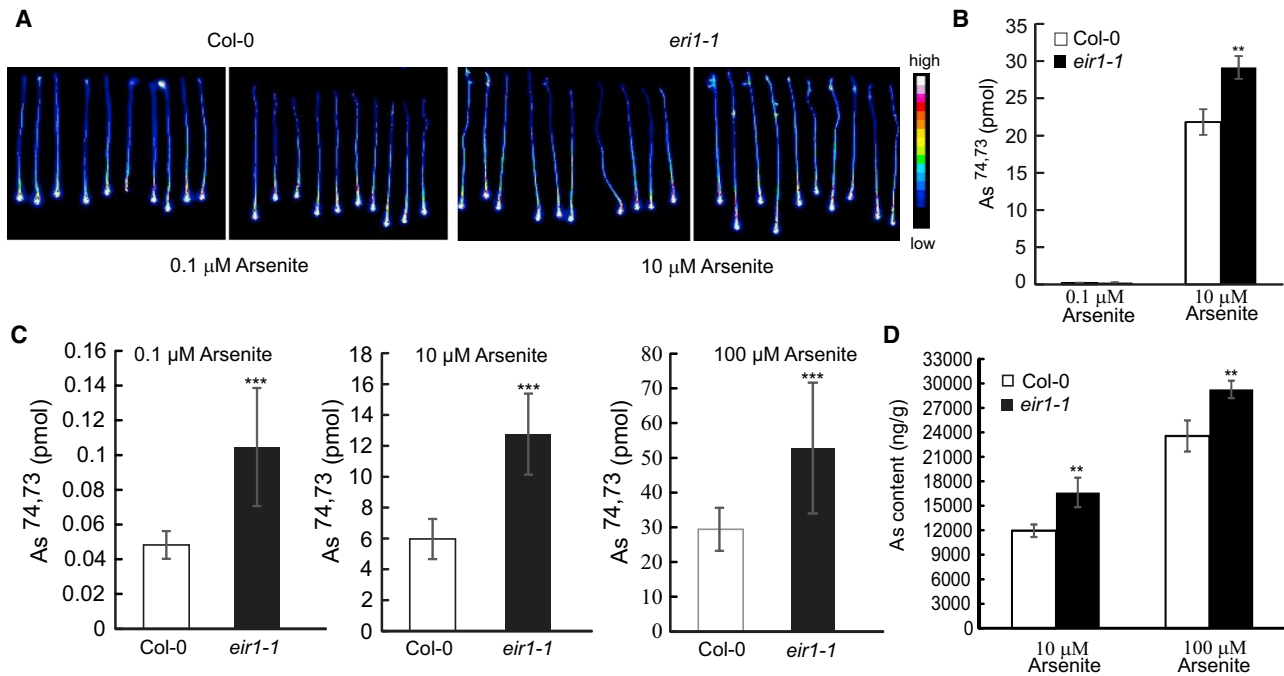


**Figure 4.** *pin2/eir1-1* Shows Altered Transport and Accumulation of Arsenite.

**(A and B)** Allocation of  $^{74,73}\text{As}$  in Col-0 and *eir1-1* **(A)**. Five-day-old Col-0 and *eir1-1* roots were incubated in 0.1  $\mu\text{M}$  and 10  $\mu\text{M}$   $^{74,73}\text{As}$  for 2 h.  $^{74,73}\text{As}$  radiation of the whole root was captured by an imaging plate. Images are representative of three independent experiments. **(B)** Quantification of As allocation in the whole root from the experiment in **(A)**. The data were obtained from three independent experiments with 10 seedling roots in each treatment. Vertical bars mean  $\pm$  SE. Asterisks represent the statistical significance between treatments as judged by Student's *t*-test: \*\**P* < 0.001.

**(C)** Scintillation counting of  $^{74,73}\text{As}$  activity in Col-0 and *eir1-1*. Five-day-old Col-0 and *eir1-1* seedlings were incubated for 2 h at 0.1, 10 and 100  $\mu\text{M}$   $^{74,73}\text{As}$ . Whole root was collected after the incubation.  $^{74,73}\text{As}$  activity of the whole root was measured by liquid scintillation counting. The data were obtained from 10 individual roots for each treatment. Vertical bars represent mean  $\pm$  SD. Asterisks represent the statistical significance between treatments as judged by Student's *t*-test: \*\*\**P* < 0.0001.

**(D)** Arsenic content in Col-0 and *eir1-1*. Five-day-old light-grown Col-0 and *eir1-1* seedlings were transferred to 10  $\mu\text{M}$  and 100  $\mu\text{M}$  arsenite solution and incubated for 2 h. A 5-mm root tip of 20 seedlings for each treatment was used to measure As by ICP-MS. The data were obtained from three independent experiments. Vertical bars represent mean  $\pm$  SE. Asterisks represent the statistical significance between treatments as judged by Student's *t*-test: \*\**P* < 0.001 and \*\*\**P* < 0.0001.

A reliable method to test for transport activity of a plant protein involves direct transport assays *in planta*. For arsenite, this is a challenging issue because labeled tracers are not commercially available. We solved the problem by generating radioactive arsenite ( $^{74,73}\text{As}$ ) by chemical reduction of radioactive arsenic (see [Supplemental Methods](#) for detailed explanation). A short-term  $^{74,73}\text{As}$  transport assay (2 h) was performed to compare arsenite transport activity in wild-type and *pin2/eir1-1* seedlings using radioimaging. Five-day-old wild-type and *pin2/eir1-1* seedlings were incubated in the presence of 0.1 and 10  $\mu\text{M}$   $^{74,73}\text{As}$  for 2 h. The quantification of radioimaged plates revealed a noticeable increase in  $^{74,73}\text{As}$ -derived signals in *pin2/eir1-1* roots when compared with wild-type roots ([Figure 4A](#) and [4B](#)), suggesting that arsenite transport is altered in *pin2/eir1-1*.

To further substantiate the results from radioimaging, we also performed a direct scintillation counting experiment using individual roots. A noticeable increase in  $^{74,73}\text{As}$  activity was observed in *pin2/eir1-1* roots for all arsenite concentrations tested ([Figure 4C](#)). Due to the low specific activity of  $^{74,73}\text{As}$ , analysis of the radioactive tracer distribution was conducted on whole plant roots. However, PIN2 is preferentially expressed in

the meristem and elongation zone ([Xu and Scheres, 2005](#); [Shibasaki et al., 2009](#)). To further confine our  $^{74,73}\text{As}$  tracer analysis, we determined radioactive arsenic distribution in 5-mm-long root tip segments after short-term (2 h) arsenite treatment using ICP-MS. Compared with wild-type, we observed an almost 1.5-fold increase in arsenic accumulation in *pin2/eir1-1* mutant plants ([Figure 4D](#)). Similar results were obtained upon long-term (3 days) arsenite treatment ([Supplemental Figure 9](#)). Collectively, these results suggest that active arsenite removal from the interior of the cells is impaired upon loss of PIN2, which might be caused by indirect effects of arsenite efflux activities due to altered auxin homeostasis. Alternatively, our results could argue for a direct involvement of PIN2 in arsenic transport across plasma membrane boundaries into the cellular exterior.

#### PIN2 Is Incapable of Transporting Arsenite in *ycf1Δ acr3Δ* Deletion Mutant of *S. cerevisiae*

The heterologous expression system is another approach by which to assess the transporter activity of proteins. Besides the bacterial arsenite transporters ArsB, AtPINs exhibit homology (18%) to arsenite transporters Acr3 from *S. cerevisiae* ([Table 1](#)).

## Plant Communications

Arsenite export by Acr3p is one of the most important arsenic detoxification mechanisms discovered in *S. cerevisiae* (Ghosh et al., 2002). Another protein mediating arsenite resistance of yeast, Ycf1p, is located at the vacuolar membrane. Ycf1p, a member of the multidrug resistance (MRP) group of the ABC superfamily of drug resistance ATPases, mediates the active transport of glutathione-conjugated toxic compounds, including the product of arsenite sequestration, As(GS)<sub>3</sub>, into yeast vacuole (Ghosh et al., 2002).

Hence, for testing the arsenite transport activity of PIN2, we selected a yeast strain lacking both Acr3p and Ycf1p (*ycf1Δ acr3Δ*). Expression of Acr3 in *ycf1Δ acr3Δ* did result in increased resistance to arsenite in the growth assay and reduced accumulation of arsenite in the transport assay. However, similar experiments performed with PIN2 expressed in yeast did not result in any arsenite transport activity (Supplemental Figure 10). Thus, while it seems reasonable to speculate about the participation of PIN2 in arsenite transport in plants, our heterologous transport assay remained inconclusive in that respect, calling for further experimental modifications.

### High-Resolution Mapping and Speciation of Arsenic in Plant Roots by Synchrotron X-Ray Fluorescence Imaging

Given the apparent aberrations in <sup>74,73</sup>As distribution in *pin2/eir1-1* mutant roots, we aimed at qualitative and quantitative assessments of the differences observed. High-resolution synchrotron X-ray fluorescence imaging coupled with XAS is a powerful technique to identify the localization and chemical speciation of metals and metalloids *in situ* (Pickering et al., 2000). In this study, application of the synchrotron techniques pursued the following goals: (1) to compare the patterns of arsenic distribution and its relative concentrations in the roots of arsenite-exposed wild-type and *pin2/eir1-1* mutant plants; and (2) to determine the chemical speciation of arsenic accumulated in the different tissues of wild-type and mutant plants by using micro-XAS and bulk XAS techniques.

Since the short-term and long-term treatments with exogenous arsenite essentially caused similar effects on PIN2 trafficking (Figure 3 and Supplemental Figure 8) and arsenic accumulation (Figure 4D and Supplemental Figure 9), in the synchrotron experiments we used long-term (3 days) arsenite-treated plants to simplify plant transportation.

Synchrotron XFI imaging revealed a striking difference in arsenite localization when comparing wild-type and *pin2/eir1-1* roots (Figure 5A and 5B). While arsenic accumulated at the very end of the root tip of arsenite-exposed *pin2/eir1-1* mutant, the arsenic distribution turned out to be more dispersed in the root apical meristem of wild-type (Figure 5A and 5B). Calculations of arsenic areal densities in comparable portions of the apical root meristem of arsenite-exposed wild-type and *pin2/eir1-1* root samples using XFI maps revealed 2- to 3-fold higher mean values for arsenic in *pin2/eir1-1* root tips compared with wild-type (Table 2, Supplemental Figure 11, and Figure 5F). These results are consistent with the observed difference in accumulation of arsenic in wild-type and *pin2/eir1-1* root tips and whole roots determined by ICP-MS (Figure 4D and

## PIN2, a Putative As(III) Transporter

Supplemental Figure 9), supporting the notion that mutations in PIN2 lead to altered arsenic distribution and root growth responses in *Arabidopsis*.

The results of principal component analysis and least-square fitting of linear components of near-edge As-K bulk XAS conducted on fresh flash-frozen leaves and roots of *eir1-1/pin2* and wild-type demonstrated that the majority of the arsenic is best represented by the As(III)-tris-thiolate complex (Supplemental Figure 12). A similar thiolate complex was observed in arsenate-exposed Indian mustard (*Brassica juncea*), which belongs to the Brassicaceae as *A. thaliana*, indicating that As-thiolates represent a major form of As deposition in this plant family (Pickering et al., 2000).

Micro-XAS analysis of As K-edge (near-edge spectra) was conducted with various parts of the roots, as shown in Figure 5C. Figure 5D demonstrates that generally much higher accumulation of arsenic in the root apex tissues of *eir1-1/pin2* seedlings compared with wild-type. The normalized and background-subtracted near-edge As K micro-XAS spectra, corresponding to the points shown in Figure 5C, were analyzed similarly to the bulk XAS. Consistent with bulk XAS results, the near-edge As K micro-XAS collected at the selected As “hot-spots” in the apical meristem of *eir1-1/pin2* and wild-type plants are best represented by the compound with As(III)-tris-thiolate coordination (Figure 5E).

The XFI elemental maps at the micrometer and submicrometer scales allowed us to compare accumulation of arsenic and other relevant trace elements in the root apical meristem of *pin2/eir1-1* and wild-type (Table 2). Root tips of arsenite-exposed *pin2/eir1-1* showed a 2- to 3-fold higher arsenic accumulation compared with the wild-type root tips. For other elements such as Fe, Zn, and Ca, no large differences in accumulation were observed between wild-type and *pin2/eir1-1* (Table 2 and Supplemental Figure 11). Collectively, these results are consistent with the findings obtained by the radioactive arsenite transport assay and ICP-MS measurements, and demonstrate that arsenic accumulates at higher levels in root meristem of *pin2/eir1-1*.

## DISCUSSION

In this work, we provide new insights into the role of the auxin efflux carrier PIN2 in regulating root arsenite response as well as in facilitating the intracellular distribution of As(III) species in roots. Several lines of molecular and cellular evidence suggest that response of *Arabidopsis* root to arsenite but not arsenate is tightly linked to an altered intracellular auxin homeostasis, regulated by PIN2. Consistently, *pin2* loss-of-function mutant seedlings exhibit striking phenotypic changes in the root morphology, and accumulated 2- to 3-fold higher arsenic concentrations in root apices compared with wild-type seedlings. The arsenite response in roots was found to be linked to an altered auxin homeostasis. Specifically, arsenite treatment produced increased reporter activity in root meristem, a hallmark feature of mutants deficient in shootward auxin transport (Luschnig et al., 1998; Ottensschläger et al., 2003), suggesting that elevated arsenite levels cause altered auxin homeostasis via targeting polar auxin transport in root meristems.

## PIN2, a Putative As(III) Transporter

## Plant Communications

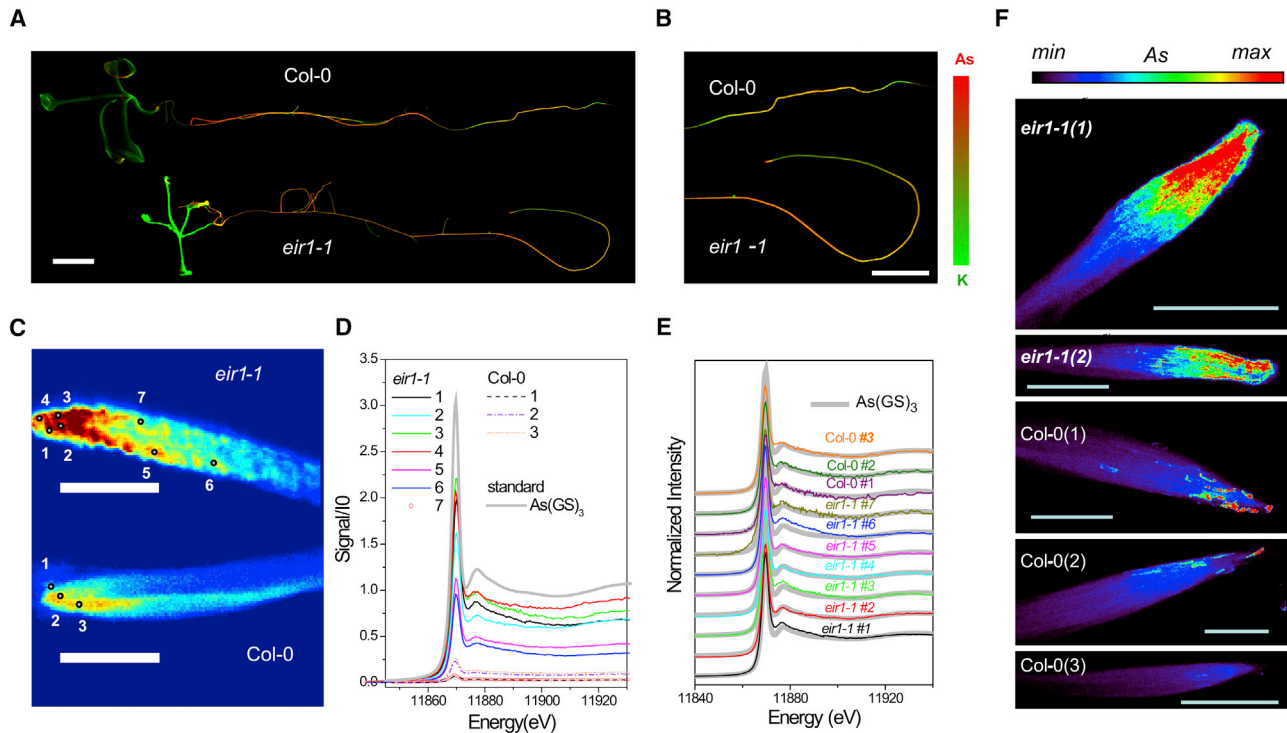


**Figure 5. As Accumulation and Distribution in *Arabidopsis* Roots Exposed to 10  $\mu$ M Arsenite are Influenced by PIN2.**

**(A)** Combined XFI As and potassium (K) elemental distributions in whole *Arabidopsis* plants. As is denoted by red and K by green, with brighter colors corresponding to higher concentrations. As (and K) intensities are on a common scale for two specimens. The samples were scanned with 35- $\mu$ m steps at beamline 10-2 (SSRL). Spatial scale bar represents 3.5 mm.

**(B)** The images of roots shown in **(A)** are magnified by 1.4 times to show differences in the As distribution in the apical part in the root meristem in Col-0 and *eir1-1/pin2*.

**(C)** High-resolution As XFI maps of the apical root meristem demonstrate higher accumulation of As in *eir1-1/pin2* and less concentrated and more dispersed distribution in Col-0. Arsenic intensity is on a common scale for two specimens. Brighter colors correspond to higher concentrations. The circular markers denote spatial points that were selected for collection of As micro-XAS in roots. The samples were scanned with 2- $\mu$ m steps at beamline 2-3 (SSRL). Spatial scale bar represents 100  $\mu$ m.

**(D)** Micro-XAS As-K near-edge spectra collected at the points of the apical root meristem in Col-0 (marked by thin dotted lines) and *eir1-1/pin2* roots as labeled in **(C)**. The spectra are normalized by intensity of the incident radiation but otherwise are not processed. Apart from *eir1-1/pin2* #7 (marked by small red empty circles), micro-XAS As-K spectra in *eir1-1/pin2* are much more intense compared with Col-0.

**(E)** Same near-edge XAS As-K spectra as in **(D)**, collected in the root points shown in **(C)**, with background removed, normalized by the intensity of the incident radiation and the edge jump. All these spectra show a high similarity to As(III)-thiolated species, best represented by As(GS)<sub>3</sub> standard.

**(F)** High-resolution XFI As areal density distributions in hydrated root specimens of *Arabidopsis* collected at beamline 2-ID-E (APS) with spatial resolution 1  $\mu$ m  $\times$  1  $\mu$ m.

BFA treatment revealed effects on the sorting of PIN2 in response to arsenite arguing for As-induced disturbance of mediators of intracellular PIN2 targeting. These effects appear to be specific, as no comparable responses could be observed when determining combinatorial effects of BFA and arsenite on intracellular dynamics of PIN1 and LTI6b reporter lines, both of which have been demonstrated to be BFA responsive (Geldner et al., 2001; Kurup et al., 2005; Shibasaki et al., 2009). On first sight, it appears paradoxical that arsenite specifically targets the intracellular cycling of PIN2 although PIN1 and PIN2 show high homology. However, this is not inconsistent, as PIN1 and PIN2 use distinct pathways for trafficking and cellular targeting (Krecek et al., 2009). For instance, in roots of *A. thaliana*, PIN1 is expressed only in the central cell files, where it always shows a polarization toward the rootward domain of the plasma membrane (Geldner et al., 2001). On the other hand, PIN2 is expressed in the LRC cells, epidermis, and cortex with a mixed polarity. In the LRC, epidermis, and mature cortical cells, PIN2

shows a polarization toward the shootward domain of plasma membrane as opposed to PIN1 polarization, while in meristematic cortical cells it shows rootward polarization like PIN1 (Rahman et al., 2007, 2010). The subcellular targeting mechanisms of PIN1 and PIN2 are also distinct. Newly synthesized non-polar PIN1 and meristematic cortical PIN2 achieve the rootward polarity through ARF-GEF, such as GNOM, and the phosphorylation status of the protein, which is regulated by the counterbalancing activities of PINOID kinase and protein phosphatase 2A. Rootward polarity of PIN1 and cortical PIN2 can be reversed to shootward by altering the phosphorylation status of the protein through overexpression of PID kinase or by reducing the protein phosphatase activity through genetic or pharmacological approaches (Friml et al., 2004; Michniewicz et al., 2007; Kleine-Vehn and Friml, 2008; Rahman et al., 2010). However, PIN1 and meristematic cortical PIN2 showed differential phosphorylation requirements for relocalization toward the shootward domain (Rahman et al.,

Plant/zone	As (ng/cm <sup>2</sup> )			Fe (ng/cm <sup>2</sup> )			Zn (ng/cm <sup>2</sup> )			Ca (ng/cm <sup>2</sup> )		
	Mean	Median	SD	Mean	Median	SD	Mean	Median	SD	Mean	Median	SD
<b><i>eir1-1</i> + 10 μM Arsenite</b>												
Z1	5252	5354	2891	1714	1539	1029	815	845	362	11 291	11 078	5103
Z2	4927	4730	2208	892	638	795	1199	1200	368	12 693	12 593	4328
<b><i>eir1-1</i> + 10 μM Arsenite</b>												
Z1	3093	2953	2218	901	836	490	619	602	433	11 090	11 705	6673
Z2	3460	3368	2278	986	899	476	587	552	404	10 843	10 861	6545
<b>Col-0 + 10 μM Arsenite</b>												
Z1	1750	1163	2381	1197	885	1092	489	517	231	13 418	13 894	4453
Z2	1068	730	1670	873	720	771	543	565	249	13 142	13 660	4568
<b>Col-0 + 10 μM Arsenite</b>												
Z1	1208	1134	1337	634	621	327	509	505	274	10 640	10 047	5661
Z2	940	838	549	672	654	304	678	691	248	13 091	12 782	5160
<b>Col-0 + 10 μM Arsenite</b>												
Z1	856	835	334	1424	1394	545	665	655	212	12 215	11 679	4015
Z2	535	483	356	1269	1272	617	638	carefully	276	9882	9716	4640
<b>Col-0 Control</b>												
Z1	7	0	14	1272	1161	749	504	501	237	11 925	11 730	4963
Z2	7	1	14	1331	1274	587	775	737	313	18 797	18 409	7027
<b><i>eir1-1</i> Control</b>												
Z1	6	0	30	1189	971	858	265	223	240	7701	6545	5225
Z2	4	0	21	764	640	669	219	187	217	4609	3800	3808

**Table 2. Areal Densities of As, Fe, Zn, and Ca.**

The statistical data for areal density was calculated from the elemental maps obtained from 2-ID-E images of Col-0 and *eir1-1/pin2* in the presence or absence of 10 μM arsenite. The ordering of the samples treated with arsenite corresponds to the ordering of images shown in Figure 5F and Supplemental Figure 12. The SD listed for each element in this case is the measure of inhomogeneity of elemental concentrations pixel-by-pixel calculated for each zone.

Z1 denotes the areas of root apical meristems.

Z2 denotes the area of transition zone plus root apical meristems.

2010). Moreover, polarization of PIN2 in LRC and in epidermal cells is completely independent of this pathway (Friml et al., 2004; Rahman et al., 2010; Hanzawa et al., 2013). Our observations, demonstrating arsenite-induced interference with the sorting of apically targeted PIN2, thus argues for arsenite effects that are specific for components controlling exocytic sorting and/or (re)cycling of PIN2. Elevated activity of auxin-responsive reporters would be consistent with such arsenite effects, specifically affecting shootward auxin transport in *Arabidopsis* root meristem.

*In planta* transport assays, together with ICP-MS and high-resolution synchrotron fluorescence imaging coupled with micro-XAS of meristems, provide evidence that arsenite efflux in *A. thaliana* is linked to the function of PIN2. It is important to note that the *in planta* transport assays and ICP-MS analyses were performed after a quite brief incubation period (2 h), which argues against any long-term indirect effects of *pin2/eir1-1* mutation in regulating arsenite distribution. The highest As accumulation areas in the elemental maps of *pin2/eir1-1* mutants obtained by synchrotron XFI were in the root cap and epidermis of apical meristem, the same cell files where PIN2 is expressed in wild-type. Moreover, while the arsenic content is altered in *pin2/*

*eir1-1*, we did not observe any striking alterations of other elements such as Fe, Zn, and Ca. This specific increased accumulation of arsenite in the root tip clearly rules out the possibility of any pleiotropic phenotype of PIN2 mutation affecting the movement/sensitivity of other inorganic ions and demonstrates the importance of PIN2 in cellular arsenite efflux.

Although our results suggest a direct involvement of PIN2 in cellular arsenite efflux, an alternative hypothesis for altered arsenite responses and accumulation in *pin2/eir1-1* could be the indirect effects of an altered auxin homeostasis on arsenite transport activities not related to PIN2. In an earlier report, the increased arsenite sensitivity of root growth upon loss of the *Arabidopsis* AUX1 auxin influx carrier or upon chemical inhibition of auxin influx as well as efflux was attributed to the change in cellular ROS-mediated signaling (Krishnamurthy and Rathinasabapathi, 2013). Mechanisms by which such an indirect effect of auxin homeostasis on arsenic responses could be brought about, however, remained entirely elusive. Furthermore, in this work they claimed that both *pin1* and *pin2* showed a hypersensitive response to arsenite-induced root growth inhibition, although we did not find any effect of arsenite on PIN1 either in the root growth or in trafficking assays. We also found several other

## PIN2, a Putative As(III) Transporter

discrepancies in this work. For instance, the authors claimed that exogenous IAA treatment alleviates arsenite tolerance in *aux1*, which is not explainable because numerous studies showed that *aux1* is IAA resistant and IAA uptake is significantly reduced in *aux1* (Pickett et al., 1990; Marchant et al., 1999; Rahman et al., 2001). The authors also claimed that arsenite inhibits auxin uptake. However, the authors performed acropetal and basipetal transport experiments, which are completely different from the auxin uptake experiment and do not truly represent the auxin uptake status of the root (Rashotte et al., 2000, 2001; Lewis et al., 2007; Shibasaki et al., 2009; Hanzawa et al., 2013). The only substantial difference in these two works was the plant growth condition; while they used an alternating light/dark regime, we used continuous light. Hence, the results presented by Krishnamurthy and Rathinasabapathi (2013) should be interpreted with caution.

In many species, removal of arsenite from the cytoplasm is mainly regulated by energy-coupled systems. In bacteria and yeast, ATP-coupled ArsAB, and H<sup>+</sup>-coupled ArsB and Acr3, function in active extrusion of arsenite (Yang et al., 2012). ArsB can also function as a subunit of the ArsAB As(III)-translocating ATPase, an ATP-driven efflux pump. In this complex, As(III) binding to three thiols of ArsA induces a conformational change that increases the rate of ATP hydrolysis and, consequently, the rate of As(III) extrusion by the ArsAB pump. The transmembrane domains of PIN proteins are remarkably similar to arsenite transporters from a range of organisms, including Sc ACR3, Pv ACR3, and arsB. Therefore, it is tempting to speculate about PINs acting in the transport of arsenite as well. However, transport assays performed with PIN2 in baker's yeast gave no indications for such PIN2 activities. This finding is not uncommon, as the outcome of heterologous expression of plant proteins varies extensively, and in many cases plant proteins are either not expressed at all or lack any functionality (Dreher et al., 2006; Ma et al., 2008; Barbosa et al., 2018). This, for example, is also true for Lsi2, a rice silicon efflux transporter implicated in the cellular efflux of arsenite, which lacks any arsenite transport activity upon expression in *Xenopus* oocytes, yeast, or bacteria (Ma et al., 2008). The authors suggested that toxic arsenite effects or restricted availability due to chemical modifications might be responsible for this lack of Lsi2 activity, and a similar scenario could be envisioned for heterologously expressed PIN2.

PINs have been shown to interact with members of the PGP/ABC family (ATP-binding cassette transporters of the B subfamily) membrane transporter family protein, which in many organisms are involved in active efflux of various xenobiotics, including metals (Blakeslee et al., 2007; Zazimalová et al., 2010; Cho et al., 2012; Maciaszczyk-Dziubinska et al., 2012; Geisler et al., 2017). Remarkably, interactions between either ABCB19 and PIN1 or ABCB1/ABCB4 and PIN2 occur at distinct plasma membrane domains, suggesting that such crosstalk is relevant for auxin transport across the plasma membrane (Blakeslee et al., 2007; Titapiwatanakun et al., 2009; Cho et al., 2012). Thus, while members of the ABCB and PIN families function as distinct auxin transport catalysts, "a strict co-operative or mutual functionality" cannot be excluded (Geisler et al., 2017). Perhaps a similar interaction between PIN2 and a so far elusive *Arabidopsis* ABCB protein is required for efficient directional transport of arsenite, which could explain our failure to demonstrate PIN2-

## Plant Communications

mediated arsenic transport in yeast. Testing of additional experimental setups and alternative heterologous systems to study properties of PIN2 as a transporter of trivalent arsenicals will be a topic of our future research.

Unlike cellular uptake of arsenite in plants, which is largely understood, efflux mechanisms as well as root responses to arsenite remain enigmatic. The findings of our present study, indicating that PIN2 and auxin are intrinsically involved in the regulation of arsenite responses in roots, and that PIN2 functions as a possible arsenite efflux transporter, open new doors to new experiments addressing arsenite responses in plants. Specifically, future studies aimed at identification of substrates that are effluxed by PIN2 or Lsi2 by means of structural nuclear magnetic resonance, and elucidating the substrate binding domains in these proteins, will greatly contribute to our understanding of the arsenite efflux mechanism in higher plants.

## METHODS

### Plant Materials

All lines except *pin1-3* (Ler background [Bennett et al., 1995]) and EGPP-LTI6b (C24 background [Kurup et al., 2005]) are in the Columbia background of *A. thaliana* (L.). *eir1-4*, *eir1-4 PIN2::PIN2*, and *eir1-4 35S::PIN2* were described earlier (Abas et al., 2006; Retzer et al., 2017). *PIN2-GFP* (Xu and Scheres, 2005) was the gift of B. Scheres (University of Utrecht, the Netherlands); DII-VENUS (Brunoud et al., 2012) was a gift from Malcolm Bennett (University of Nottingham, UK). *pin1-3*, *pin3-4*, *pin4-3*, and GFP-LTI6b were provided by Gloria Muday (Wake Forest University, Winston-Salem, NC, USA). Columbia-0 (Col-0), *eir1-1*, and PIN1-GFP were obtained from the Arabidopsis Biological Resource Center (Columbus, OH, USA).

### Growth Conditions

Surface-sterilized seeds were germinated and grown for 5 days in modified Hoagland medium containing 1% (w/v) sucrose and 1% (w/v) agar (Difco Bacto agar, BD Laboratories; <http://www.bd.com>) in a growth chamber (NK system, LH-70CCFL-CT, Japan) at 23°C under continuous white light (at an irradiance of 80–100 μmol m<sup>-2</sup> s<sup>-1</sup>; Shibasaki et al., 2009). The seedlings were grown vertically for 5 days and then transferred to new plates with or without arsenite and arsenate, and incubated for various lengths of time under continuous light at irradiance of 80–100 μmol m<sup>-2</sup> s<sup>-1</sup> (NK system, LH-1-120.S, Japan). After the incubation, pictures of the seedlings were taken using a digital camera (Canon Power Shot A 640; <http://canon.jp>) and root elongation of the seedlings was analyzed by the image-analysis software ImageJ (<http://rsb.info.nih.gov/ij/>). *pin1-3* was maintained as heterozygous, and homozygous seedlings were selected using the fused cotyledon phenotype as described earlier (Aida et al., 2002).

### Chemicals

Sodium (meta) arsenite (NaAsO<sub>2</sub>) and sodium arsenate dibasic heptahydrate (Na<sub>2</sub>HAsO<sub>4</sub>·7H<sub>2</sub>O) were purchased from Kanto Chemical (Tokyo, Japan). BFA was purchased from Sigma-Aldrich Chemical (USA). [<sup>3</sup>H] IAA (20 Ci mmol<sup>-1</sup>) was purchased from American Radiolabeled Chemicals (St. Louis, MO, USA; <http://www.a-rc-inc.com>). The chemicals for growth media and standards used in synchrotron experiments were purchased from Sigma-Aldrich (Canada). Other chemicals were from Wako Pure Chemical Industries (<http://www.wako-chem.co.jp/>).

### Bioinformatics Analysis

Protein sequences of AtPIN1 (AT1G73590), AtPIN2 (AT5G57090), AtPIN3 (AT1G70940), AtPIN4 (AT2G01420), and AtPIN7 (AT1G23080) were collected from TAIR ([www.arabidopsis.org](http://www.arabidopsis.org)). *Saccharomyces cerevisiae*

## Plant Communications

Acr3 (190409919), *Pteris vittata* Acr3 (310768536), *Escherichia coli* arsenite transporter ArsB (1703365), and *Oryza sativa* silicon transporter Lsi2 (296936086) were collected from the NCBI ([www.ncbi.nlm.nih.gov](http://www.ncbi.nlm.nih.gov)) protein database. Multiple sequence alignment (Supplemental Figures 2 and 3) and identity matrix (Table 1 and Supplemental Tables 1–3) were generated using the Clustal Omega (Sievers et al., 2011) (<http://www.ebi.ac.uk/Tools/msa/clustalo/>) multiple sequence alignment tool. Cladograms of plasma membrane-residing PIN proteins (AtPIN1, AtPIN2, AtPIN3, AtPIN4, AtPIN7) (Supplemental Figure 1) from *A. thaliana* were constructed using MEGA6 (Molecular Evolutionary Genetics Analysis) (Tamura et al., 2013) software based on neighbor-joining method and 1000-bootstrap test.

### Gravitropism Assay

Root tip reorientation was assayed as described earlier (Rahman et al., 2010). In brief, 5-day-old vertically grown seedlings were transferred to new square plates in the presence or absence of arsenite. After the transfer, the roots were gravistimulated at 23°C by rotating the plate 90°. To measure the curvature of roots and elongation, we took photographs of plates at specific time points after reorientation using a digital camera (Canon Power Shot A 640) and analyzed them using image-analysis software ImageJ. Data were obtained from three biological replicates.

### Transport Assays

#### Auxin Transport Assay

Five-day-old vertically grown *Arabidopsis* seedlings were transferred to agar plates and incubated with or without 10 μM arsenite for 3 days. Shootward auxin transport was measured as described earlier (Shibasaki et al., 2009). In brief, a donor drop was prepared by mixing 0.5 μM [<sup>3</sup>H]IAA (3.7 MBq ml<sup>-1</sup>) in 1.5% agar containing MES buffer solution. The donor drop was placed on the edge of the root tip. Plates were then incubated vertically at 23°C for 2 h. For measurement of auxin transport, 5-mm root segments away from the apical 2 mm were carefully cut and soaked overnight in 4 ml of liquid scintillation fluid (Ultima Gold, PerkinElmer, USA), and the radioactivity was measured with a scintillation counter (model LS6500, Beckman ACSII; USA Instruments, Fullerton, CA). Data were obtained from at least three biological replicates.

#### Arsenite Transport Assay

<sup>74,73</sup>As(III) prepared from radioactive arsenic (<sup>74,73</sup>As) was used for transport assay. The <sup>74,73</sup>As(III) preparation method is described in detail in Supplemental Methods. Five-day-old vertically grown Col-0 and *eir1-1* seedlings were incubated in Hoagland solution containing 0.1 and 10 μM labeled <sup>74,73</sup>As(III) (approximately 5 kBq ml<sup>-1</sup>) for 2 h and transferred to a fresh plate to separate root and shoot samples. For radioluminography, the seedling roots were incubated in 0.1 and 10 μM and then placed on a Kraft paper using double-sided tape. The sample was exposed to an imaging plate (BASIP MS, GE Healthcare Lifescience) and the radiation distribution was visualized by an FLA-5000 Image Analyzer (Fujifilm). Arsenic contents in seedlings were calculated from the value of photostimulated luminescence in the imaging data. Data were obtained from three biological replicates.

For the liquid scintillation count, individual whole root samples were taken in separate tubes and 10 individual roots were considered for each treatment. Individual root samples were collected in vials with scintillation cocktail (Microscint 40, PerkinElmer) and <sup>74,73</sup>As activity was measured by a liquid scintillation counter (Tri-Carb 4810 TR, PerkinElmer) with the window of 0–2000 keV.

### Live Cell Imaging and GUS Staining

For live cell microscopy, 5-day-old GFP or DII-VENUS transgenic seedlings were used. For short-term BFA treatment, 5-day-old seedlings were incubated in 10 μM arsenite for 2 h and then subjected to 20 μM BFA for 40 min. For long-term treatment, 5-day-old seedlings were incubated with or without 10 μM arsenite for an additional 3 days. After the in-

## PIN2, a Putative As(III) Transporter

cupation, BFA treatment was performed as described above. After the BFA incubation, the seedlings were mounted in liquid growth medium on a coverglass for observation on a Nikon laser scanning microscope (Eclipse Ti equipped with Nikon C2 Si laser scanning unit) and imaged with a 40× water immersion objective.

The accumulation of BFA bodies in PIN2-GFP was quantified in the transition area of the root tip as described earlier (Shibasaki et al., 2009). The pictures were taken approximately at the same place on the root using the same confocal settings. The number of BFA bodies and cells were counted for each root and expressed as BFA body/cell. Data were obtained from at least three biological replicates. DII-VENUS imaging and GUS staining are described in Supplemental Methods.

### Measurement of Arsenic Content in Plants

For short-term treatment, 5-day-old wild-type and *pin2/eir1-1* seedlings were transferred to Hoagland solution containing 10 μM and 100 μM arsenite and incubated for 2 h. After incubation, roots were washed three times with reverse-osmosis water, and 5 mm of root tip was cut, dried, and weighed. Twenty root tips were collected into a vial. After digestion by nitric acid, As content in the sample solution was measured by inductively coupled plasma mass spectrometry (ICP-MS) (NexION 350S, PerkinElmer). For long-term treatment, 5-day-old seedlings were treated for 3 days in arsenite-spiked agarose growth medium and As content in roots and shoots was measured as described above.

### Expression of PIN2 in *ycf1Δ acr3Δ* Mutant of *S. cerevisiae*

Since arsenite resistance in *S. cerevisiae* is largely mediated by Acr3p and Ycf1p, we used the yeast strain lacking both Ycf1p and Acr3p (*ycf1Δ acr3Δ*). PIN2 and Acr3p were cloned in pKT10 vector, transformed into the double-knockout strain, and selected with AHCW/Glc medium. Preparation of double-knockout strain, cloning of PIN2 and Acr3p, and growth and transport assays are described in detail in Supplemental Methods.

### X-Ray Fluorescence Imaging and X-Ray Absorption Spectroscopy

Synchrotron XFI was performed at the Stanford Synchrotron Radiation Lightsource (SSRL), Stanford University, Menlo Park, CA, USA (beamlines 10-2 and 2-3) and at the Advanced Photon Source (APS), Argonne National Laboratory, Lemont, IL, USA (beamline 2-ID-E). Micro-XAS analysis of selected arsenic hot spots in the samples at room temperature was performed at beamline 2-3 of SSRL, and bulk As K-edge XAS of frozen plant tissues and growth medium was conducted in a helium cryostat environment at beamline 7-3 of SSRL.

### Preparation of Samples for Synchrotron XFI Imaging

*Col-0* and *pin2/eir1-1* were grown as described above. Five-day-old seedlings were treated with 10 μM arsenite in growth medium for 3 days. After the treatment, control and arsenite-exposed plants were harvested, washed in deionized water, and either flash-frozen for consecutive bulk XAS analysis or imaged as described below and, in more detail, in Supplemental Methods.

### XFI of Whole Plants

Elemental mapping of whole plants using XFI was performed at the wiggler beamline 10-2 (SSRL). The samples were mounted at 45° to the incident beam and raster scanned (pixel size 35 μm × 35 μm) with beam dwell time 100 ms per pixel (Supplemental Figure 13; see Supplemental Methods for details). Fluorescent energy windows were centered for As, Fe, and other elements of interest (P, S, K, Ca, Zn, Cu, and Mn).

### Micro-XFI and Micro-XAS of Selected Plant Tissues

Higher-resolution imaging (2–10 μm) of selected tissues of interest (areas of the apical root meristem of live main roots) were performed at the bending magnet beamline 2-3 (SSRL) with the same geometric and



## Plant Communications

## PIN2, a Putative As(III) Transporter

- Indriolo, E., Na, G., Ellis, D., Salt, D.E., and Banks, J.A.** (2010). A vacuolar arsenite transporter necessary for arsenic tolerance in the arsenic hyperaccumulating fern *Pteris vittata* is missing in flowering plants. *Plant Cell* **22**:2045–2057.
- Kamiya, T., Tanaka, M., Mitani, N., Jian, F.M., Maeshima, M., and Fujiwara, T.** (2009). NIP1;1, an aquaporin homolog, determines the arsenite sensitivity of *Arabidopsis thaliana*. *J. Biol. Chem.* **284**:2114–2120.
- Kleine-Vehn, J., and Friml, J.** (2008). Polar targeting and endocytic recycling in auxin-dependent plant development. *Annu. Rev. Cell Dev. Biol.* **24**:447–473.
- Krecke, P., Skupa, P., Libus, J., Naramoto, S., Tejos, R., Friml, J., and Zazimalová, E.** (2009). The PIN-FORMED (PIN) protein family of auxin transporters. *Genome Biol.* **10**:249.
- Krishnamurthy, A., and Rathinasabapathi, B.** (2013). Auxin and its transport play a role in plant tolerance to arsenite-induced oxidative stress in *Arabidopsis thaliana*. *Plant Cell Environ.* **36**:1838–1849.
- Kurup, S., Runions, J., Köhler, U., Laplace, L., Hodge, S., and Haseloff, J.** (2005). Marking cell lineages in living tissues. *Plant J.* **42**:444–453.
- Latowski, D., Kowalczyk, A., Nawieśniak, K., and Listwan, S.** (2018). Arsenic uptake and transportation in plants. In *Mechanisms of Arsenic Toxicity and Tolerance in Plants*, M. Hasanuzzaman, K. Nahar, and M. Fujita, eds. (Singapore: Springer Nature), pp. 1–26.
- Laxmi, A., Pan, J., Morsy, M., and Chen, R.** (2008). Light plays an essential role in intracellular distribution of auxin efflux carrier PIN2 in *Arabidopsis thaliana*. *PLoS One* **3**:e1510.
- Lee, D.A., Chen, A., and Schroeder, J.I.** (2003). *ars1*, an *Arabidopsis* mutant exhibiting increased tolerance to arsenate and increased phosphate uptake. *Plant J.* **35**:637–646.
- Lewis, D.R., Miller, N.D., Splitt, B.L., Wu, G., and Spalding, E.P.** (2007). Separating the roles of acropetal and basipetal auxin transport on gravitropism with mutations in two *Arabidopsis* multidrug resistance-like ABC transporter genes. *Plant Cell* **19**:1838–1850.
- Luschign, C., Gaxiola, R.A., Grisafi, P., and Fink, G.R.** (1998). EIR1, a root-specific protein involved in auxin transport, is required for gravitropism in *Arabidopsis thaliana*. *Genes Dev.* **12**:2175–2187.
- Ma, J.F., Yamaji, N., Mitani, N., Xu, X.-Y., Su, Y.-H., McGrath, S.P., and Zhao, F.-J.** (2008). Transporters of arsenite in rice and their role in arsenic accumulation in rice grain. *Proc. Natl. Acad. Sci. U S A* **105**:9931–9935.
- Maciaszczyk-Dziubinska, E., Wawrzycka, D., and Wysocki, R.** (2012). Arsenic and antimony transporters in eukaryotes. *Int. J. Mol. Sci.* **13**:3527–3548.
- Mansour, N.M., Sawhney, M., Tamang, D.G., Vogl, C., and Saier, M.H.** (2007). The bile/arsenite/riboflavin transporter (BART) superfamily. *FEBS J.* **274**:612–629.
- Marchant, A., Kargul, J., May, S.T., Muller, P., Delbarre, A., Perrot-Rechenmann, C., and Bennett, M.J.** (1999). AUX1 regulates root gravitropism in *Arabidopsis* by facilitating auxin uptake within root apical tissues. *EMBO J.* **18**:2066–2073.
- Meharg, A.A., and Zhao, F.J.** (2012). *Arsenic & Rice* (Dordrecht: Springer).
- Michniewicz, M., Zago, M.K., Abas, L., Weijers, D., Schweighofer, A., Meskinec, I., Heisler, M.G., Ohno, C., Zhang, J., Huang, F., et al.** (2007). Antagonistic regulation of PIN phosphorylation by PP2A and PINOID directs auxin flux. *Cell* **130**:1044–1056.
- Nietzold, T., West, B.M., Stuckelberger, M., Lai, B., Vogt, S., and Bertoni, M.I.** (2018). Quantifying X-ray fluorescence data using MAPS. *J. Vis. Exp.* **132**:e56042.
- Okada, K., Ueda, J., Komaki, M., Bell, C., and Shimura, Y.** (1991). Requirement of the auxin polar transport system in early stages of *Arabidopsis* floral bud formation. *Plant Cell* **3**:677–684.
- Ottenschläger, I., Wolff, P., Wolverson, C., Bhalerao, R.P., Sandberg, G., Ishikawa, H., Evans, M., and Palme, K.** (2003). Gravity-regulated differential auxin transport from columella to lateral root cap cells. *Proc. Natl. Acad. Sci. U S A* **100**:2987–2991.
- Pickering, I.J., Prince, R.C., George, M.J., Smith, R.D., George, G.N., and Salt, D.E.** (2000). Reduction and coordination of arsenic in Indian mustard. *Plant Physiol.* **122**:1171–1177.
- Pickett, F.B., Wilson, A.K., and Estelle, M.** (1990). The *aux1* mutation of *Arabidopsis* confers both auxin and ethylene resistance. *Plant Physiol.* **94**:1462–1466.
- Rahman, A., Ahamed, A., Amakawa, T., Goto, N., and Tsurumi, S.** (2001). Chromosaponin I specifically interacts with AUX1 protein in regulating the gravitropic response of *Arabidopsis* roots. *Plant Physiol.* **125**:990–1000.
- Rahman, A., Bannigan, A., Sulaman, W., Pechter, P., Blancaflor, E.B., and Baskin, T.I.** (2007). Auxin, actin and growth of the *Arabidopsis thaliana* primary root. *Plant J.* **50**:514–528.
- Rahman, A., Takahashi, M., Shibasaki, K., Wu, S., Inaba, T., Tsurumi, S., and Baskin, T.I.** (2010). Gravitropism of *Arabidopsis thaliana* roots requires the polarization of PIN2 toward the root tip in meristematic cortical cells. *Plant Cell* **22**:1762–1776.
- Rashotte, A.M., Brady, S.R., Reed, R.C., Ante, S.J., and Muday, G.K.** (2000). Basipetal auxin transport is required for gravitropism in roots of *Arabidopsis*. *Plant Physiol.* **122**:481–490.
- Rashotte, A.M., DeLong, A., and Muday, G.K.** (2001). Genetic and chemical reductions in protein phosphatase activity alter auxin transport, gravity response, and lateral root growth. *Plant Cell* **13**:1683–1697.
- Ravenscroft, P., Brammer, H., and Richards, K.** (2009). *Arsenic Pollution: A Global Synthesis* (Chichester: Wiley-Blackwell).
- Retzer, K., Lacek, J., Skokan, R., Del Genio, C.I., Vosolsobě, S., Laňková, M., Malinská, K., Konstantinova, N., Zazimalová, E., Napier, R.M., et al.** (2017). Evolutionary conserved cysteines function as cis-acting regulators of *Arabidopsis* PIN-FORMED 2 distribution. *Int. J. Mol. Sci.* **18**:2274.
- Salt, D.E.** (2017). Would the real arsenate reductase please stand up? *New Phytol.* **215**:926–928.
- Shen, S., Li, X.-F., Cullen, W.R., Weinfeld, M., and Le, X.C.** (2013). Arsenic binding to proteins. *Chem. Rev.* **113**:7769–7792.
- Shibasaki, K., Uemura, M., Tsurumi, S., and Rahman, A.** (2009). Auxin response in *Arabidopsis* under cold stress: underlying molecular mechanisms. *Plant Cell* **21**:3823–3838.
- Sievers, F., Wilm, A.A., Dineen, D., et al.** (2011). Fast, scalable generation of high-quality protein multiple sequence alignments using Clustal Omega. *Mol Syst Biol* **7**:539.
- Simon, S., Skupa, P., Viaene, T., Zwiewka, M., Tejos, R., Klíma, P., Carná, M., Rolčík, J., De Rycke, R., Moreno, I., et al.** (2016). PIN6 auxin transporter at endoplasmic reticulum and plasma membrane mediates auxin homeostasis and organogenesis in *Arabidopsis*. *New Phytol.* **211**:65–74.
- Song, W.-Y., Yamaji, N., Ko, D., Jung, K.-H., Fujii-Kashino, M., An, G., Martinoia, E., Lee, Y., and Ma, J.F.** (2014). A rice ABC transporter, OsABCC1, reduces arsenic accumulation in the grain. *Proc. Natl. Acad. Sci. U S A* **111**:15699–15704.
- Tamura, K., Stecher, G., Peterson, D., Filipowski, A., and Kumar, S.** (2013). MEGA6: molecular evolutionary genetics analysis version 6.0. *Mol. Biol. Evol.* **30**:2725–2729.

## PIN2, a Putative As(III) Transporter

## Plant Communications

**Titapiwatanakun, B., Blakeslee, J.J., Bandyopadhyay, A., Yang, H., Mravec, J., Sauer, M., Cheng, Y., Adamec, J., Nagashima, A., Geisler, M., et al.** (2009). ABCB19/PGP19 stabilises PIN1 in membrane microdomains in *Arabidopsis*. *Plant J.* **57**:27–44.

**Wan, Y., Jasik, J., Wang, L., Hao, H., Volkmann, D., Menzel, D., Mancuso, S., Baluška, F., and Lin, J.** (2012). The signal transducer NPH3 integrates the phototropin1 photosensor with PIN2-based polar auxin transport in *Arabidopsis* root phototropism. *Plant Cell* **24**:551–565.

**Wu, D., Shen, H., Yokawa, K., and Baluška, F.** (2015). Overexpressing OsPIN2 enhances aluminium internalization by elevating vesicular trafficking in rice root apex. *J. Exp. Bot.* **66**:6791–6801.

**Xu, J., and Scheres, B.** (2005). Dissection of *Arabidopsis* ADP-RIBOSYLATION FACTOR 1 function in epidermal cell polarity. *Plant Cell* **17**:525–536.

**Xu, W., Dai, W., Yan, H., Li, S., Shen, H., Chen, Y., Xu, H., Sun, Y., He, Z., and Ma, M.** (2015). *Arabidopsis* NIP3;1 plays an important role in arsenic uptake and root-to-shoot translocation under arsenite stress conditions. *Mol. Plant* **8**:722–733.

**Yang, H.C., Fu, H.L., Lin, Y.F., and Rosen, B.P.** (2012). Pathways of arsenic uptake and efflux. *Curr. Top. Membr.* **69**:325–358.

**Zazimalová, E., Murphy, A.S., Yang, H., Hoyerová, K., and Hosek, P.** (2010). Auxin transporters—why so many? *Cold Spring Harb. Perspect. Biol.* **2**:a001552.